Am J Transl Res 2024;16(5):1643-1659
www.ajtr.org /ISSN:1943-8141/AJTR0156345

Original Article

Dynamic mRNA network profiles in macrophages challenged with lipopolysaccharide

Li Chen[1,2*], Lei Li[3*], Chenyang Huang[1*], Xusong Cao[1], Yong Jiang[1,4]

[1]Guangdong Provincial Key Laboratory of Proteomics, State Key Laboratory of Organ Failure Research, Department of Pathophysiology, School of Basic Medical Sciences, Southern Medical University, Guangzhou 510515, Guangdong, China; [2]Department of Anesthesiology, The Third Affiliated Hospital of Southern Medical University, Southern Medical University, Guangzhou 510630, Guangdong, China; [3]Department of Neurology, Shenzhen Hospital of Southern Medical University, Shenzhen 518000, Guangdong, China; [4]Department of Respiratory and Critical Care Medicine, The Tenth Affiliated Hospital, Guangdong Provincial Key Laboratory of Proteomics, Southern Medical University (Dongguan People's Hospital), Dongguan 523059, Guangdong, China. [*]Equal contributors and co-first authors.

Received March 5, 2024; Accepted April 18, 2024; Epub May 15, 2024; Published May 30, 2024

Abstract: Objectives: To elucidate the transcriptome of macrophages in an inflammation model induced by lipopolysaccharide (LPS), providing insight into the molecular basis of inflammation. Methods: We utilized RNA sequencing (RNA-seq) to analyze dynamic changes in gene expression in RAW264.7 macrophages treated with LPS at multiple time points. Differentially expressed genes (DEGs) were identified using the edgeR package. Short Time-series Expression Miner (STEM) and KEGG pathway enrichment analyses were conducted to determine temporal expression patterns during inflammation. Results: We identified 2,512 DEGs, with initial inflammatory responses occurring in two distinct phases at 1 h and 3 h. Venn diagram analysis revealed 78 consistently dysregulated genes throughout the inflammatory process. A key module of 18 dysregulated genes was identified, including Irg1, which may exert an inhibitory effect on inflammation. Further, a second metabolic shift in activated macrophages was observed at the late middle stage (12 h). Multi-omics analysis highlighted the ribosome's potential regulatory role in the inflammatory response. Conclusions: This study provides a detailed view of the molecular mechanisms underlying inflammation in macrophages and reveals a dynamic genetic landscape crucial for further research. Our findings underscore the complex interaction between gene expression, metabolic shifts, and ribosomal functions in response to LPS-induced inflammation.

Keywords: Macrophage, transcriptome, metabolism, inflammation

Introduction

According to the Third International Consensus Definitions for Sepsis (Sepsis-3), sepsis is defined as life-threatening organ dysfunction resulting from a dysregulated host immune response to infection [1]. The underlying mechanism of sepsis involves immune dysfunction characterized by early immune system overactivation followed by late immune suppression [2]. The innate immune system, serving as the first line of defense against infections, involves key players such as neutrophils, monocytes/macrophages, dendritic cells, natural killer cells, T cells, and others, all pivotal in the pathophysiology of sepsis [3].

Macrophages, critical components of the innate immune system, play a vital role in immune homeostasis and the inflammatory response [4]. They are distributed across various tissues and perform multiple functions during all stages of sepsis, including phagocytosis, bactericidal action, antigen presentation, and secretion of inflammatory factors and chemokines [5]. In the early stages of sepsis, macrophages release a large number of pro-inflammatory factors and chemokines, such as enzymes, complement proteins, and regulatory factors like interleukin-1 (IL-1), which intensify the inflammatory response [6]. This response provides a basis for using macrophages in cell models to assess the pro-inflammatory effects of stimuli

including lipopolysaccharide (LPS) [7]. In the later stages of sepsis, excessive apoptosis of macrophages leads to immune suppression [8].

Current understanding reveals that the mechanisms governing sepsis are complex and dynamic, influenced by various microbial and host factors that trigger typical inflammatory cascades [9]. Studies have shown that pathogen-associated molecular patterns such as LPS, flagellin, muramyl dipeptide in peptidoglycan, and CpG bacterial DNA, are recognized by pattern recognition receptors of the innate immune system [6]. This recognition initiates intracellular signaling cascades crucial for inflammatory and immune responses. For instance, LPS binding to toll-like receptor 4 on immune cell membranes activates the mitogen-activated protein kinase signaling pathways by both MyD88-dependent and independent mechanisms. This activation leads to the phosphorylation and nuclear translocation of transcription factors such as nuclear factor-κB (NF-κB), activator protein-1, and interferon regulatory factor 3, which promote the expression of inflammatory cytokines in macrophages [10]. Despite significant advances in understanding sepsis pathophysiology, it remains a clinical challenge due to high mortality rates ranging from 28% to 50% [11]. Thus, a deeper comprehension of the molecular regulatory mechanisms of the inflammatory response is ineeded. We explored the mechanisms underlying the inflammatory response of macrophage challenged with LPS.

Our previous study on the proteome of macrophages treated with LPS provided insight into the sequential changes in proteins indicative of the transition from early to late stages of inflammation, suggesting a potential role for ribosomal proteins in inflammation development [12]. However, the quantitative correlation between mRNA and protein levels across various species is generally low (R2~0.01-0.5), indicating that mRNA levels alone are often insufficient to predict protein levels [13, 14]. Therefore, investigating changes in the transcriptomes of macrophages stimulated with LPS is crucial for a more comprehensive understanding of the inflammatory response.

Understanding the complex and dynamic mechanisms of sepsis requires both transcriptional and protein-level analyses of the immune response. Our previous study highlighted the proteomic landscape of macrophages challenged with LPS, revealing sequential changes in proteins and the potential role of ribosomal proteins in inflammation [15]. We observed that mRNA and protein levels do not consistently correlate across various species (R2~0.01-0.5) [16, 17]. This discrepancy underscores the importance of investigating both mRNA expression in transcriptomes and protein levels in proteomes to fully comprehend the inflammatory response.

Transcriptomics provides insight into the immediate transcriptional activity of the genome, capturing early cellular responses to stimuli such as LPS. These changes in mRNA levels are crucial for understanding the activation of signaling pathways and the ensuing cascade of events leading to inflammatory cytokine production [18-22]. However, the translation of these mRNA transcripts into functional proteins is influenced by various regulatory mechanisms, including post-transcriptional modifications, which may not be reflected solely by mRNA levels.

Proteomics, in contrast, examines the protein products of the genome and their functional roles within the cell. By analyzing the proteome, we can identify proteins differentially expressed in response to LPS stimulation, which may not be predictable based solely on mRNA data. This aspect is particularly vital for understanding the functional outcomes of the inflammatory process, as proteins are the effector molecules that mediate immune responses and cellular functions.

In this study, we utilized both transcriptomic and proteomic analyses to elucidate the molecular mechanisms underlying the inflammatory response in macrophages induced by LPS. By integrating these two approaches, we aim to bridge the gap between gene expression and protein function, thereby providing a nuanced understanding of the molecular events that drive sepsis and inflammation.

RNA sequencing (RNA-seq), a second-generation sequencing technology, has become a pivotal method for transcriptome profiling. This technique offers a significantly more precise measurement of transcript levels compared to traditional methods and has been extensively

used for gene annotation, transcript profiling, and single-nucleotide polymorphism discovery across various species [15]. Transcriptional changes of coding genes in various inflammation models have been widely explored at the genome-wide level, but sequential transcriptome analyses, particularly in LPS-induced macrophages, have been sparse [16].

We performed sequential transcriptome analysis using RNA-seq to characterize the dynamic gene expression profiles during the macrophage inflammatory response to LPS. Additionally, this study presents an integrative analysis of both the transcriptome and proteome in macrophages challenged with LPS at multiple time points. This systematic approach enhances our understanding of the comprehensive molecular mechanisms that underpin the dynamic process of inflammation and provides essential data for further investigations into macrophage responses to LPS.

Materials and methods

Cell culture and LPS treatment

RAW264.7 cells, obtained from the American Type Culture Collection (ATCC, Manassas, VA, USA), were cultured in Dulbecco's Modified Eagle's Medium (DMEM) (Cat# C11995500BT; Gibco, Grand Island, NY, USA) supplemented with 10% fetal bovine serum (FBS) (Cat# 1795588; Gibco, Grand Island, NY, USA). The cells were maintained at approximately 80% confluence, with passage numbers not exceeding ten. Cells were incubated in a humidified atmosphere containing 5% CO_2 at 37°C. The medium was refreshed every other day. For experimental treatments, RAW264.7 cells were exposed to LPS (100 ng/ml) for durations of 0, 1, 3, 6, 12, or 24 h.

Total RNA extraction

Total RNA was extracted using TriPure Isolation Reagent (Cat# A244914; Roche) following the manufacturer's instructions. Cells were washed with DPBS (Cat# C14190500BT; Gibco, Grand Island, NY, USA), lysed with 200 µL of TRIzol, and tubes were gently inverted for 5 min. Following centrifugation at 12,000×g for 15 min at 4°C, the supernatant was transferred to a new tube. An equal volume of isopropanol was added, the tubes were vigorously shaken for 15 s, and then left to stand at room temperature for 3 minutes. After a further centrifugation at 12,000×g for 10 min at 4°C, the supernatant was discarded, and the RNA pellet was washed with 75% precooled ethanol. Post-centrifugation for 5 min, the ethanol was removed, and the RNA pellet was air-dried for 5 min and resuspended in 20 µL of RNase-free water. RNA integrity was verified using the RNA Nano 6000 Assay Kit and the Bioanalyzer 2100 system (Agilent Technologies, CA, USA). RNA concentration and purity were measured using a NanoDrop spectrophotometer (Thermo Fisher Scientific, Wilmington, DE).

cDNA library preparation for RNA-seq

For each cell sample (approximately 1 million cells), 1 mL of TRIzol reagent was used for total RNA extraction according to the manufacturer's protocol. Sequencing libraries were constructed using the Sample Preparation Guide of the MGIEasy RNA Library Kit V3.0 (MGI Shenzhen, Cat#1000006384). mRNA was enriched using the Dynabeads mRNA purification protocol and fragmented into approximately 250 bp at 94°C for 8 min. This was followed by first and second strand synthesis, end repair, A-tailing, adapter ligation, and 14 cycles of PCR amplification. The PCR products were purified and quantified with the Qubit dsDNA HS Assay. A yield of 1 pmol was required for Single Strand Circularization, which was then sequenced on the MGISEQ-2000 platform for 50 cycles. The quality of the sequencing data is reported in Tables S1 and S2. RNA sequencing was performed on three independent samples of RAW264.7 cells treated with LPS for 1, 3, 6, 12, and 24 h, and 3 control samples without treatment.

Quantitative real-time PCR

Pure RNA was treated with RNase-free DNase (Cat# M6101; Promega) and reverse transcribed using the ReverTra Ace qPCR RT Kit (Cat# FSQ-101; Toyobo, Japan) in a 10 µL reaction volume following the manufacturer's instructions. Transcript quantification was performed by real-time PCR (RT-PCR) using SYBR qPCR Mix (Cat# QPK-201; Toyobo, Japan) on a 7500 Fast Real-time PCR System (Applied Biosystems, Foster City, CA). The 50 µL qPCR reaction included 25 µL of SYBR Green PCR

Master Mix, 1 μmol/L of each primer, and 12.5 μL of cDNA template. The amplification program was set as follows: 50°C for 2 min, 95°C for 10 min, followed by 40 cycles of 95°C for 15 s and 60°C for 1 min. Primers for amplifying target mRNAs (Cyp2u1, Cbx2, Irg1, Creb3l2, SPP1, and Slc15a3) were sourced from Beijing Genomics Institute (BGI) (Table S3). Data were analyzed using ABI 7500 Software (v2.0.1), and relative expression levels were calculated using the $2^{-\Delta\Delta}$CT method. Experiments were conducted in biological triplicate.

Quantification and analysis of differentially expressed genes (DEGs)

Gene expression levels were quantified using Reads Per Kilobase Million (RPKM). Differential expression analysis was conducted with the edgeR package [17]. *P*-values were adjusted using the Benjamini-Hochberg method to control the false discovery rate (FDR) [18]. Genes with an FDR ≤ 0.01 and an absolute $\log_2$(Fold Change) ≥ 2 were identified as DEGs.

Gene ontology (GO) and Kyoto Encyclopedia of Genes and Genomes (KEGG enrichment analysis)

The biological functions of DEGs were explored using GO and KEGG enrichment analyses, performed with the cluster Profiler R package [19]. Enriched terms with a *P*-value ≤ 0.05 were considered statistically significant and visualized using the ggplot2 R package [20].

Weighted gene co-expression network analysis (WGCNA)

The WGCNA R package was used to identify time trait-related gene modules [21]. Genes were clustered into different modules based on a topological overlap matrix-based dissimilarity measure, with a cut height set at 0.25, a minimal module size of 30, and a threshold of 0.3. Modules with a *P*-value ≤ 0.01 were further analyzed for biological functions using the ClueGO plug-in of Cytoscape software.

Integrative analysis of the transcriptome and proteome by "mixOmics" R package

Integrative analysis of transcriptomic and proteomic data across multiple time points was conducted using the mixOmics R package [22]. Reduced-dimensional data were further explored to understand biological functions through additional GO and KEGG enrichment analyses.

Integrative analysis of the transcriptome and proteome by "mixOmics" R package

RAW264.7 cells, sourced from the American Type Culture Collection (ATCC, Manassas, VA, USA), were cultured in DMEM (Cat# C11995500BT; Gibco, Grand Island, NY, USA) supplemented with 10% fetal bovine serum (FBS) (Cat# 1795588; Gibco). The cells were maintained in a humidified incubator at 37°C with 5% CO_2. For treatments, cells were exposed to LPS (100 ng/ml) for 0, 3, 6, 12, or 24 h. Post-treatment, cells were washed with DPBS (Cat# C14190500BT; Gibco) and lysed using 8M urea (Cat# U4883; Sigma, St. Louis, MO, USA) for protein extraction. Proteins were then digested into peptides, and peptide expression levels were quantified using liquid chromatography-tandem mass spectrometry followed by peptide library comparison. Differentially expressed proteins (DEPs) were identified based on *p*-values < 0.05 and fold changes (FC) > 1.5 relative to controls. The detailed experimental procedures are illustrated in Figure S2.

Statistical analysis

Differential expression for transcriptomics data was assessed using the Student's *t*-test, with genes considered significantly differentially expressed at a fold change (FC) ≥ 4 or ≤ 0.25 and a *FDR* ≤ 0.01. For proteomic data, proteins with an *FDR* < 0.05 and an FC > 1.5 compared to the control group were identified as significantly dysregulated.

Results

Dynamic transcriptomic response to LPS in macrophages

To understand the underlying mechanisms of macrophage response to LPS, we performed RNA-seq analyses at multiple time points. We analyzed global transcriptomic changes in RAW264.7 cells at six time points (0, 1, 3, 6, 12, and 24 h), obtaining a total of 42.07 Gb of clean data across 18 samples, with each sample providing at least 1.88 Gb of data and Q30

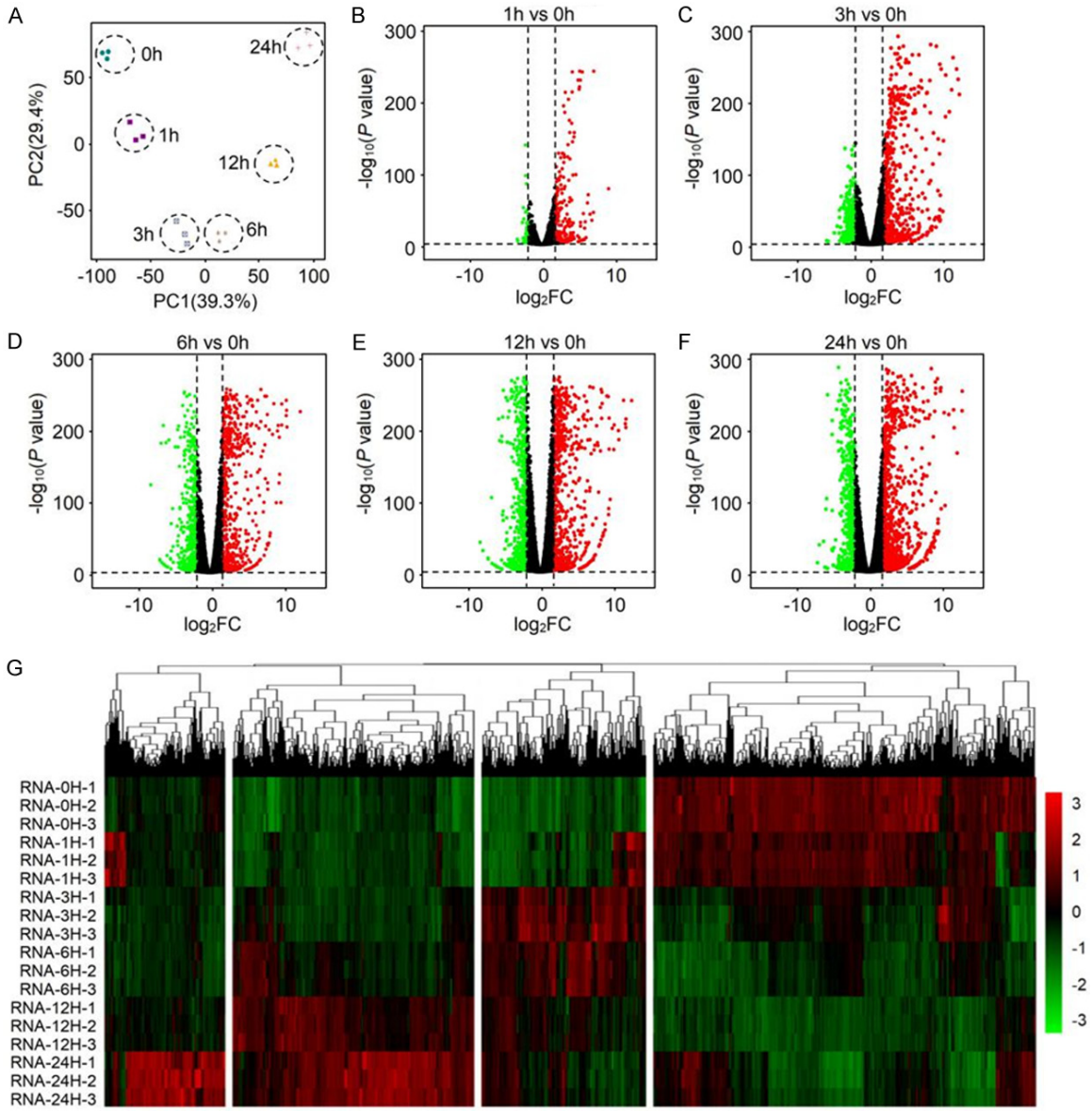

Figure 1. Transcriptomic overview of RAW264.7 cells stimulated with lipopolysaccharide (LPS) over time. A. A principal component analysis plot displays global transcriptome profiles. B-F. Volcano plots illustrate differentially expressed genes (DEGs) during LPS-induced inflammatory responses in macrophages at 1, 3, 6, 12, and 24 h compared to control. Red spots indicate up-regulated DEGs, green spots show down-regulated DEGs, and black spots represent genes with no significant changes in expression. The horizontal axis (log_2(FC)) shows the fold change of genes expressed in RAW264.7 cells treated with LPS compared to control, while the vertical axis (-log_{10}(*p*-value)) displays the log-transformed *p*-value. DEGs were identified using cut-off criteria of *p*-value ≤ 0.01 and $Log_2FC \geq 2$ or ≤ -2. G. A heatmap with hierarchical clustering dendrograms of DEGs shows responses to LPS stimulation at 0 (control), 1, 3, 6, 12, and 24 h. Red represents higher expression levels, and blue indicates lower expression levels.

quality scores exceeding 81.72% (Table S1). The total number of mapped reads per sample ranged from 13.8 to 24.6 million, achieving mapping ratios between 77.3% and 86% (Table S2).

Principal component analysis was used to assess the reproducibility and clustering of the biological replicates. Replicates from the same treatment group clustered closely, confirming the reliability of the experimental conditions. Notably, samples from different LPS treatment times were distinctly separated from each other and from control groups, highlighting significant LPS-induced changes in gene expression (**Figure 1A**).

To visualize these differences, volcano plots for RAW264.7 cells treated with LPS at different time points. We established thresholds for DEGs with a *FDR* ≤ 0.01 and a $\log_2$-fold change (Log_2FC) ≥ 2 or ≤ -2. In total, 2,512 DEGs were identified at different time points (1, 3, 6, 12 and 24 h) treated with LPS (Table S3). Specifically, 270 DEGs (222 upregulated and 48 downregulated) at 1 h, 833 DEGs (521 upregulated and 312 downregulated) at 3 h, 1,112 DEGs (572 upregulated and 540 downregulated) at 6 h, 1,311 DEGs (677 upregulated and 634 downregulated) at 12 h, and 1,487 DEGs (983 upregulated and 504 downregulated) at 24 h were identified (**Figure 1B-F**). It was observed that the late stages of LPS-induced inflammation exhibited more DEGs compared to the early stages.

Further analysis of mRNA relationships at different time points was conducted using hierarchical clustering, presented in a heatmap. This analysis revealed that LPS treatment induced more than three distinct mRNA expression patterns in RAW264.7 cells, as indicated by varying color saturation (**Figure 1G**).

Following the hypothesis that gene classes relevant to our experimental treatment should exhibit similar expression patterns, we conducted a gene expression pattern analysis using the STEM on the OmicShare tools platform, a free online platform for data analysis (www.omicshare.com/tools) [23]. This analysis retrieved 100 expression profiles, 24 of which were = significant (P ≤ 0.05) (Figure S1). These 24 significant profiles were categorized into three groups: category A consists of expression modules that generally show increased abundance at 24 h compared to 0 h, including profiles 17, 31, 39, 41, 46, 50, 52, 57, 66, 67, 76, 89, 90, 95, and 99 (**Figure 2A**); category B includes profiles that display a general decrease in abundance at 24 h compared to 0 h, including profiles 0, 6, 32, 33, 42, and 47; and category C comprises profiles t hat maintain a generally consistent abundance at 24 h compared to 0 h, including profiles 2, 34, and 65 (Figures S3, S4).

Based on the results from the KEGG pathway analysis, we identified distinct signaling pathway networks in the genes comprising the profiles of category A (**Figure 2A**). Notably, pathways involved in the inflammatory response were predominantly associated with profiles 66, 89, and 95. Genes within these profiles were upregulated during the early stages (1 h) and mid-early stage (3 h) of the inflammatory process, maintaining high levels thereafter. These profiles were significantly enriched in the JAK-STAT signaling pathway, TNF signaling pathway, NOD-like receptor signaling pathway, and interactions between viral proteins and cytokine receptors. Concurrently, pathways related to metabolism were primarily found in profile 52, where gene expression was initially unaffected by LPS treatment but later upregulated during the late middle stage (12 h) of inflammation. Enrichment analysis revealed significant involvement in glycine, serine, and threonine metabolism, biosynthesis of amino acids, and ABC transporters.

Further insights were obtained through GO enrichment analysis for the aforementioned profiles (profiles 66, 89, 95, and 52). We observed that genes in profiles 66, 89, and 95 were primarily involved in biological processes linked to the immune response, defense response, stress response, and positive regulation of immune system processes (**Figure 2B-D**). These biological processes are intricately connected to the inflammatory and immune responses. In contrast, genes in profile 52 predominantly participated in biological processes related to the transmembrane transport of amino acids, L-amino acid transport, cellular catabolic processes, and organic substance catabolism (**Figure 2E**). These findings underscore the diverse roles of these gene profiles in the cellular response to LPS stimulation.

A Venn diagram was used to investigate the dysregulated genes in macrophages during inflammation. DEGs were defined by criteria of $|\log_2(\text{fold change})| \geq 2$ and FDR ≤ 0.01 compared to the control group. Stage-specific DEGs were exclusively identified in groups treated with LPS at 1, 3, 6, 12, and 24 h, numbering 85, 156, 171, 144, and 536, respectively. A total of 78 DEGs were found to be consistently up- or down-regulated throughout the entire inflammatory process (**Figure 3A**). Notably, of these 78 genes, 76 were consistently upregulated (**Figure 3B**), while only 2 genes, Cyp2u1 and Cbx2, were consistently downregulated at all time points.

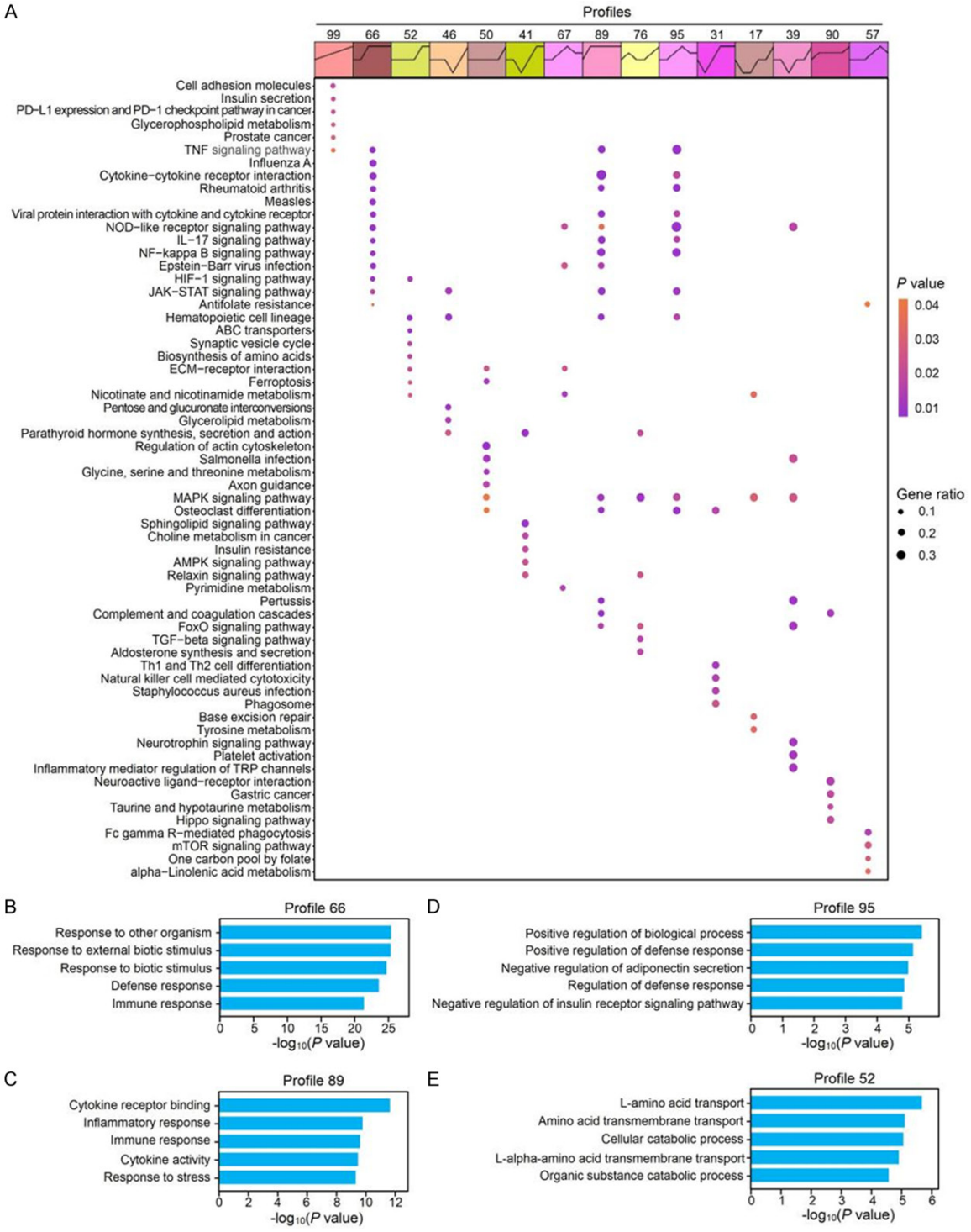

Figure 2. Overview of the global temporal changes in gene abundance within category A during the inflammatory process in macrophages challenged with lipopolysaccharide (LPS). A. The top panel depicts genes with significant changes in abundance ($P \leq 0.05$) throughout the time series. The bottom panel shows the functional enrichment analysis of KEGG pathways conducted using the "ClusterProfiler" R package. B-E. Highlight of the top 5 GO enrichment terms for profiles 66, 89, 95, and 52, identifying gene regulatory networks related to biological function.

Further GO enrichment analysis predicted the biological functions of the 76 upregulated genes. The most significantly enriched GO term was "positive regulation of cytokine produc-

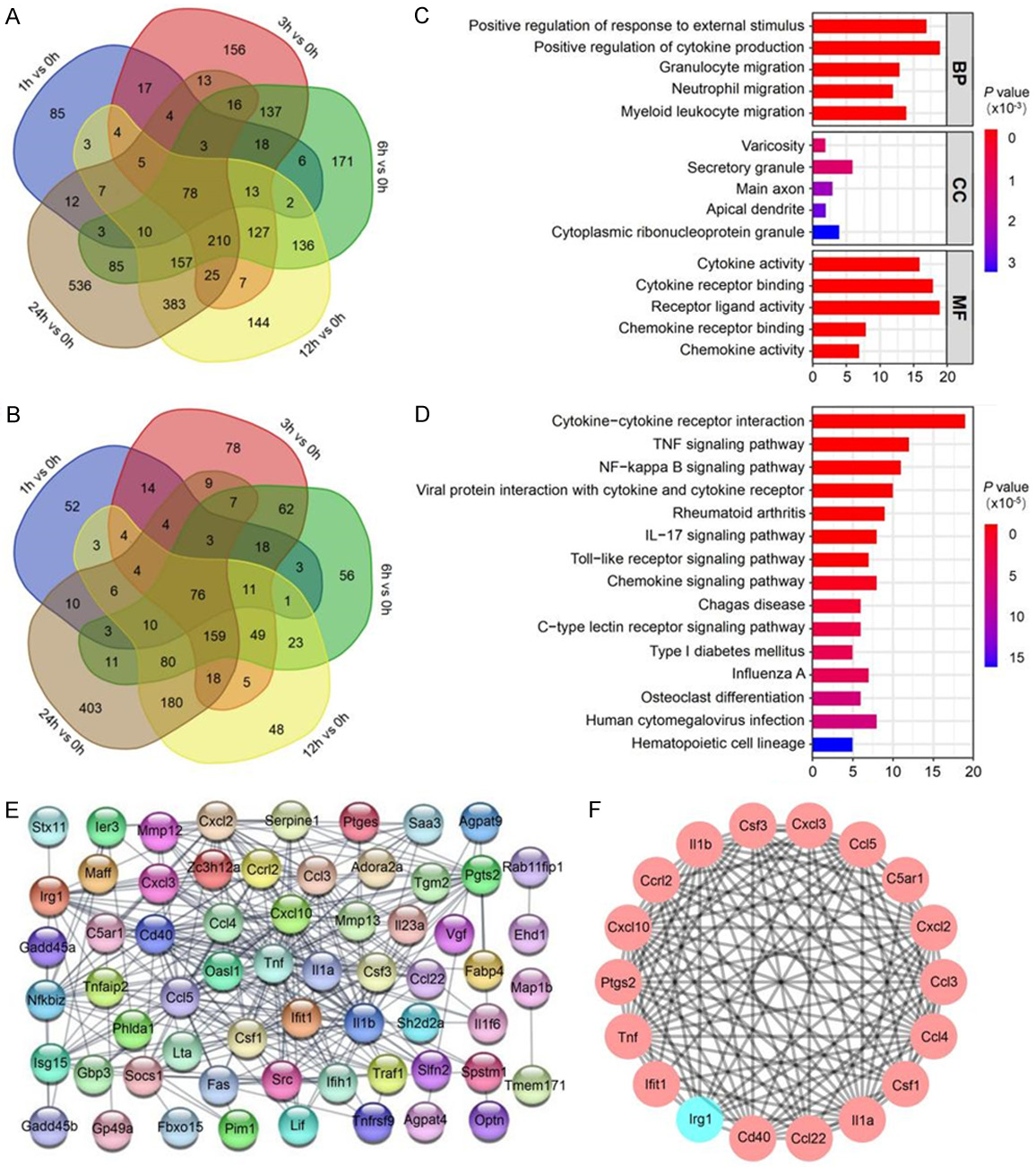

Figure 3. Comparison of DEGs during the inflammation process induced by LPS. A. Venn diagram illustrates dysregulated genes specific to various inflammatory phases or shared across all stages. B. Another Venn diagram highlights upregulated genes that are either phase-specific or consistent throughout the process. C. The 76 consistently upregulated genes were functionally annotated using GO enrichment analysis. D. KEGG pathway analysis was conducted to explore the enrichment of these 76 upregulated genes. E. STRING analysis revealed the protein-protein interaction network for these genes during inflammation. F. The MCODE plug-in of Cytoscape software identified the most significant module within the 76 upregulated genes.

tion" in biological processes, while "receptor ligand activity" was the top term in molecular functions (**Figure 3C**). KEGG enrichment analysis revealed that the most enriched pathways among these 76 genes included inflammatory and immune response-related pathways such as the TNF signaling pathway, NF-kappa B signaling pathway, and IL-17 signaling pathway

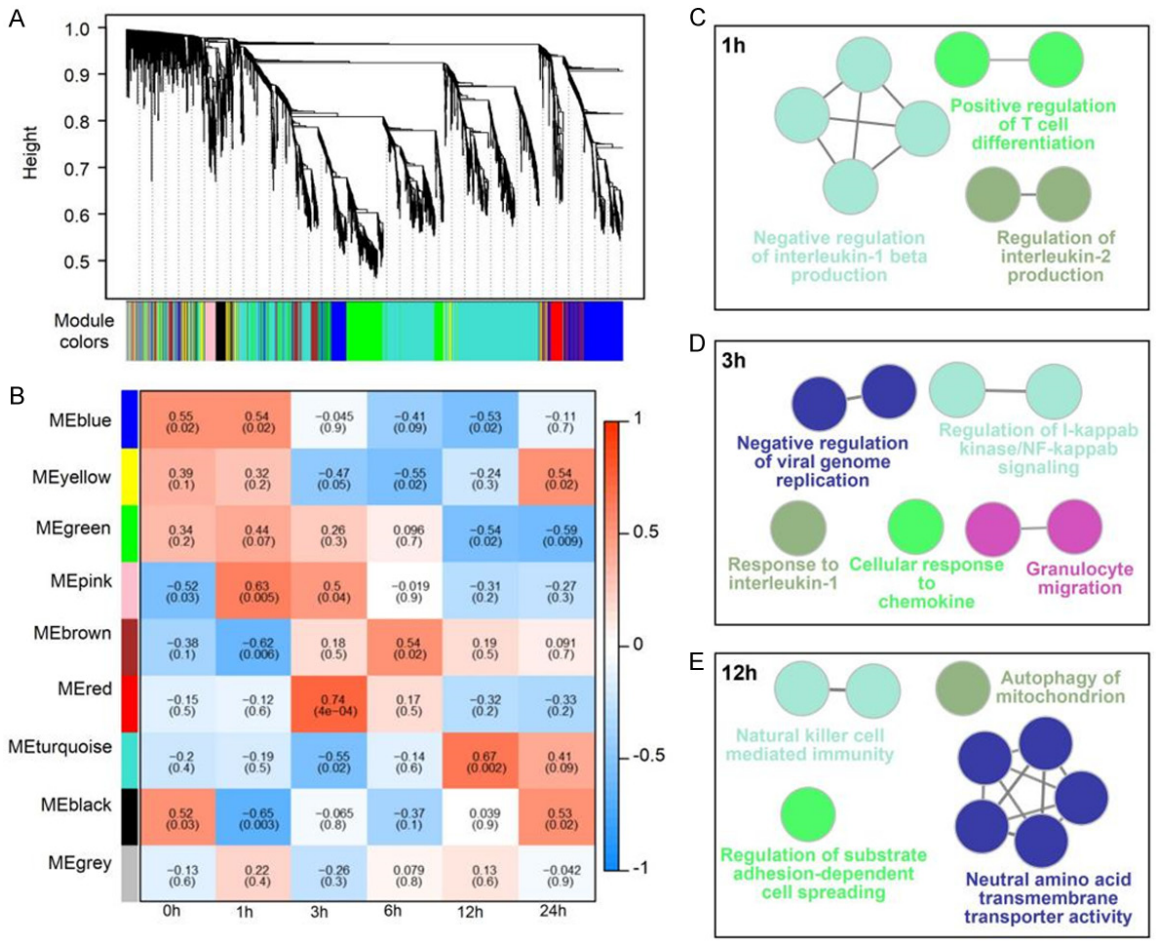

Figure 4. Weighted gene co-expression network analysis (WGCNA). A. A clustered dendrogram of the top 5000 genes using the dissimilarity measure. B. Heatmap illustrates the correlations between modules and time points, with the correlation coefficient and *P*-value included in each cell. C-E. Enrichment analyses were performed on genes within the pink, red, and turquoise modules, respectively, with a *P*-value < 0.05 to identify their biological functions.

(**Figure 3D**), underscoring the critical role of macrophages throughout the inflammatory process.

To delve deeper into the interrelationships among the 76 upregulated genes, interaction analysis was conducted using the STRING database. Most of these genes formed a tightly interconnected network (**Figure 3E**). The MCODE plug-in of Cytoscape software identified a key module comprising 18 genes, including Tnf, Il1b, Il1a, Cxcl10, Cxcl2, Ccl4, Cd40, Csf3, Ptgs2, Csf1, Ccl5, Ccl3, Cxcl3, Irg1, Ccrl2, Ccl22, C5ar1, and Ifit1 (**Figure 3F**). Notably, the majority of these genes are associated with a proinflammatory response, except for Irg1, which is implicated in inhibiting inflammation through its role in producing itaconate.

Identification of time-resolved gene modules by WGCNA

WGCNA was utilized to identify gene modules associated with different time points during the inflammatory response. Nine modules were identified using a cut height of 0.25, a minimal module size of 30, and a threshold of 0.3 (**Figure 4A**). Only modules with a *P*-value ≤ 0.01 and a correlation coefficient greater than zero were considered significant and related to specific time points. The heatmap of module-trait relationships (**Figure 4B**) identified three modules (pink, red, and turquoise) that showed significant correlations with the times at 1, 3, and 12 hours, respectively. The ClueGO plug-in of Cytoscape was used to delineate the potential biological processes of genes within these

modules. The pink module was strongly associated with positive regulation of T cell differentiation, negative regulation of interleukin-1 beta production, and regulation of interleukin-2 production (**Figure 4C**). The red module was related to the regulation of I-κB kinase/NF-κB signaling, neutrophil migration, negative regulation of viral genome replication, response to interleukin-1 and chemokines, and granulocyte migration (**Figure 4D**). The turquoise module was closely linked to regulation of neutral amino acid transmembrane transporter activity, natural killer cell-mediated immunity, regulation of substrate adhesion-dependent cell spreading, and autophagy of mitochondria (**Figure 4E**).

Integrative analysis of the transcriptome and proteome in macrophages challenged with LPS

Building on the proteomics data collected at the same time points in our previous experiment [12]. With the exception of the 1-hour time point, we employed the "mixOmics" R package for a multi-omics analysis to gain a comprehensive understanding of the biological functions during the inflammatory process in LPS-challenged macrophages. This integrative analysis aimed to identify the most significant omics variables contributing to the sepsis response. The heatmap of the multiomics signature from Principal Component 1 (PC1) revealed strong correlations between 126 dysregulated genes and 131 dysregulated proteins during sepsis (**Figure 5A**). These correlations featured positive (red modules) and negative (green modules) relationships.

To further elucidate the biological significance of these correlated genes and proteins, GO and KEGG enrichment analyses were performed. For the 126 DEGs, GO enrichment analysis highlighted their involvement in inflammation and immune response processes, such as positive regulation of defense response, leukocyte cell-cell adhesion, and response to interferon-beta (**Figure 5B**). The KEGG enrichment analysis identified the C-type lectin receptor signaling pathway as the most significantly enriched pathway (**Figure 5C**).

Interestingly, for the 131 differentially expressed proteins (DEPs), the most significantly enriched GO term and KEGG pathway were related to ribonucleoprotein complex biogenesis and ribosome, respectively (**Figure 5D**, **5E**). These findings underscore the ribosome's significant role in the inflammatory process, highlighting its involvement beyond traditional translational functions to potentially regulating inflammation in macrophages challenged with LPS.

Validation of global temporal changes in macrophages challenged with LPS by RT-PCR for mRNA analysis

Six genes were randomly selected to validate the gene expression profiles obtained by sequencing. The genes included Cyp2u1, Cbx2, Irg1, Creb3l2, Spp1, and Slc15a3 (**Figure 6A-L**). The expression profiles of these genes were consistent with their sequencing results, thereby substantiating the reliability of our data.

Discussion

We utilized RNA-seq technology to explore the temporal dynamics of gene expression in RAW264.7 cells treated with LPS, with the aim of elucidating the mechanisms driving inflammation. RNA-seq is notably sensitive for detecting gene expression levels, especially in low-abundance transcripts, and does not require prior knowledge of gene sequences, unlike microarrays [24]. This represents the first application of time-resolved transcriptome profiling to investigate the molecular mechanisms and regulatory networks involved in LPS-induced inflammatory responses in macrophages.

The inflammatory process is intricately regulated through a series of signaling events by key pathway regulators [25]. Although changes in inflammation are gradual, distinct phases marking critical events suggest significant shifts during its progression. To identify potential key phases, we performed STEM analysis, identifying 24 statistically significant profiles ($P \leq 0.05$) (Figure S1). Subsequent KEGG enrichment analysis of these profiles (particularly 66, 89, and 95) highlighted their strong association with inflammatory response pathways (**Figure 2A**). GO enrichment analysis further confirmed that these profiles are predominantly linked to inflammation and immune responses, including terms like inflammatory response, positive regulation of defense response, and response to external biotic stimulus (**Figure 2B-D**).

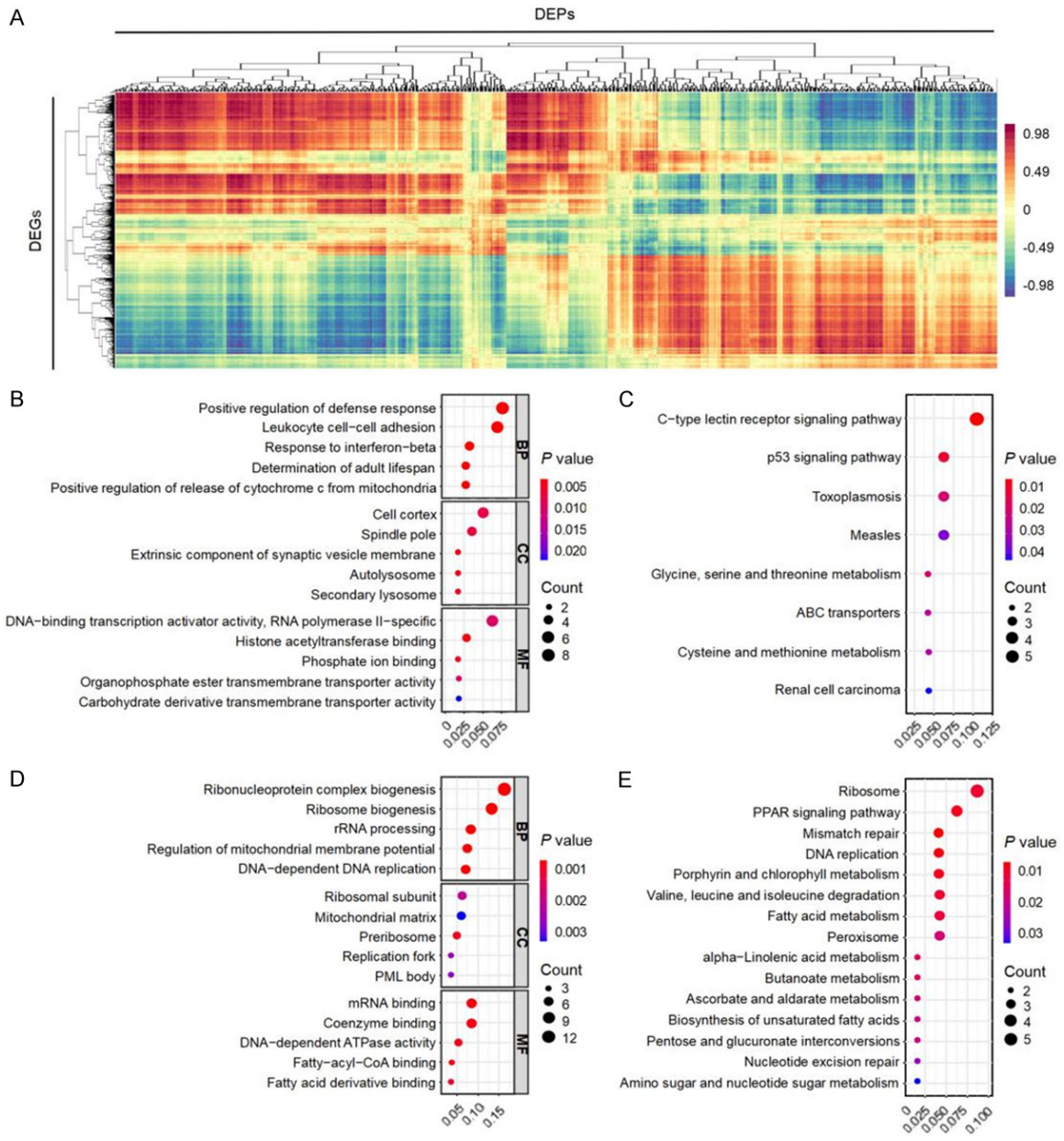

Figure 5. Integrative analysis of the transcriptomics and proteomics datasets in the process of inflammation. A. Hierarchical clustering for canonical correlation analysis was conducted on genes and proteins. The mixOmics R package was employed to compute pairwise correlations between mRNA abundance (rows) and protein abundance (columns). B, C. GO and KEGG enrichment analyses determined the enriched terms for significantly dysregulated genes identified in the PC1. D, E. Similarly, enriched terms for significantly dysregulated proteins identified in the principal component 1 were determined through GO and KEGG enrichment analyses.

Our results also indicate that genes associated with inflammation are primarily upregulated in the early stage (1 h) and mid-early stage (3 h) of the inflammatory process. For instance, genes such as IL1a, Tnf, Cxcl1, and IL1b are upregulated within the first hour, while IL6 and Ccl2 show increased expression at the three-hour mark. Interestingly, previous studies have shown that IL6 levels rise more slowly than TNF levels in macrophage cultures stimulated with LPS [26], corroborating our findings. These observations suggest that the onset of inflammation can be divided into two distinct phases: an initial rapid response within the first hour

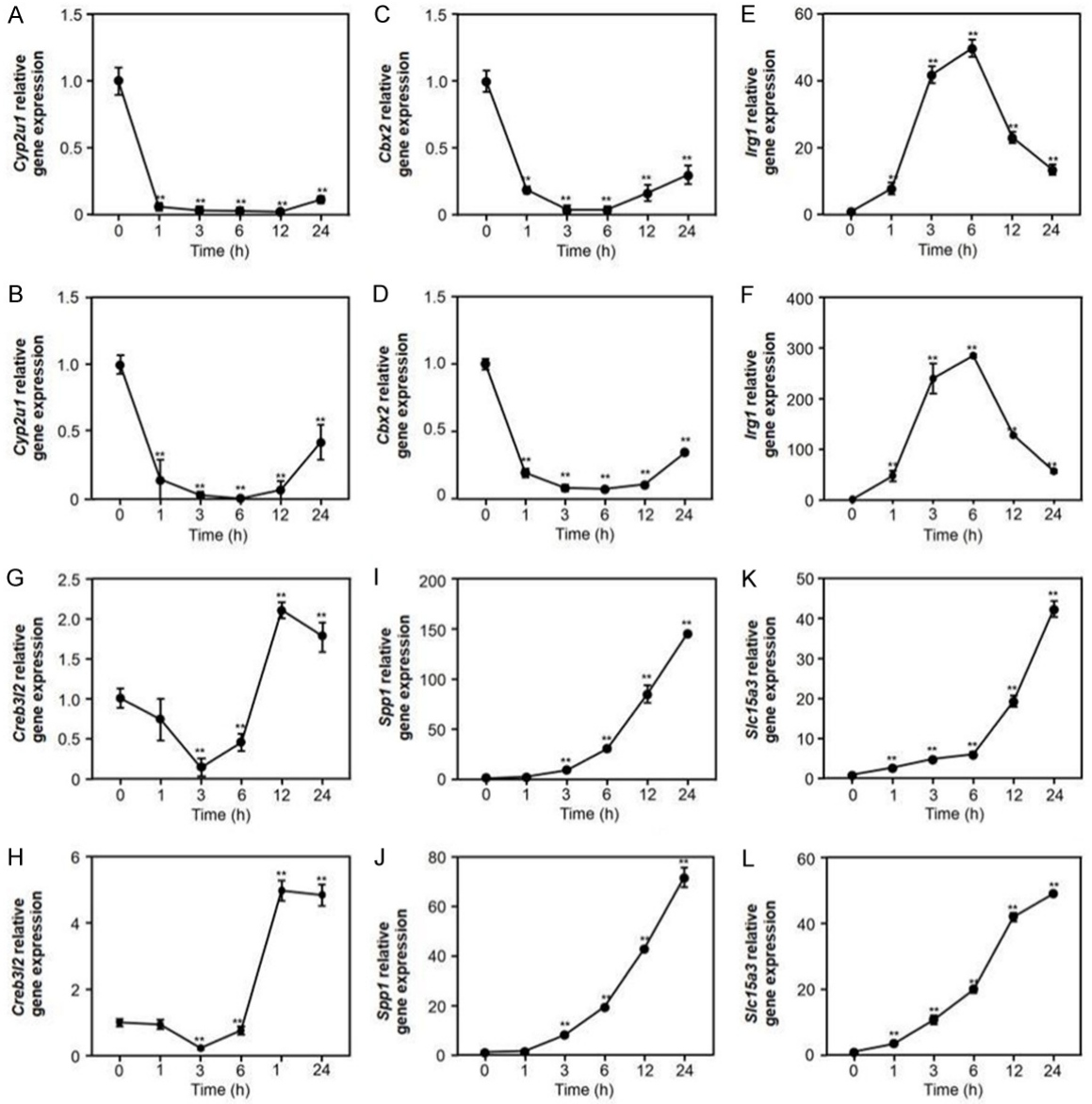

Figure 6. Validation of the differential expression of 6 candidate genes (Cyp2u1, Cbx2, Irg1, Creb3l2, Spp1 and Slc15a3) through quantitative real-time PCR (RT-PCR). RT-PCR analysis was performed using total RNA isolated from RAW264.7 cells treated with LPS (100 ng/mL) at 0, 1, 3, 6, 12, and 24 h. The fold change in mRNA was determined by normalizing the data against the average value of the control group. Gene expression levels were normalized to β-actin transcript levels. The results from RT-PCR (up) are consistent with those from RNA-seq (down) for all six candidate genes. (A, B) Cyp2u1, (C, D) Cbx2, (E, F) Irg1, (G, H) Creb3l2, (I, J) Spp1, (K, L) Slc15a3. Relative gene expressions were normalized by comparison with β-actin expression and analyzed using the $2^{-\Delta\Delta CT}$ method, with three biological replicates (n = 3). $^{**}P < 0.01$.

and a subsequent amplification phase around three hours later, marking an expansion of the inflammatory response.

Previous studies have highlighted the crucial role of metabolism in macrophage function. Under normal physiologic conditions, macrophages predominantly utilize oxidative phosphorylation (OXPHOS) to meet their energy needs through glucose metabolism [27]. However, when macrophages encounter pathogens or inflammatory agents such as lipopolysaccharide (LPS) and cytokines (e.g., TNF-α, IL-1), they undergo metabolic reprogramming, shifting from OXPHOS to glycolysis [28]. This metabolic shift enables the synthesis of ATP mole-

cules necessary to meet the heightened energy demands of combating pathogens and inflammogens [29]. The activation of macrophages is therefore critically supported by changes in metabolism, and the immunoregulatory functions of macrophages are directly influenced by their metabolic state. Disruption of these metabolic processes can impair proper macrophage activation [30].

In our current study, KEGG pathway enrichment analysis identified that metabolism-related pathways were predominantly associated with profile 52, where genes were significantly upregulated at 12 hours (**Figure 2A**). Consistent with these findings, GO enrichment analysis showed significant enrichment for terms related to amino acid transport and catabolic processes within this profile (**Figure 2B-E**). These results indicate a substantial alteration in macrophage metabolism in response to LPS challenge at the 12-hour mark.

Additionally, we observed an increase in the AMP-activated protein kinase (AMPK) signaling pathway at 12 h in profile 41 (**Figure 2A**). Previous research has established that AMPK acts as a critical regulator of cellular energy metabolism, promoting catabolic processes that enhance the capacity of cells to oxidize fatty acids, amino acids, and glucose, thereby efficiently generating ATP through the electron transport chain (ETC) [31]. AMPK is typically activated by an increasing ADP (or AMP) to ATP ratio, suggesting that the metabolic changes observed at 12 h may be attributable to the activation of the AMPK pathway [31]. During the inflammatory response of macrophages treated with LPS, the ratio of ADP (or AMP) to ATP gradually increases, potentially triggering the AMPK pathway in the late middle stage (12 h) of inflammation. Activation of this pathway would promote catabolic metabolism, thereby enhancing the ability of macrophages to oxidize substrates to fuel the ETC and generate ATP.

Furthermore, we found distinctively enriched GO terms in other profiles. For instance, profile 50 showed enrichment for terms including entry into host cell, viral entry into host cell, positive regulation of angiogenesis, and positive regulation of vasculature development, among others (Figure S4). The genes in this profile were upregulated in the late stage (24 h), suggesting that late-stage gene changes in macrophages may facilitate the resolution of inflammation by promoting the removal of necrotic tissue and supporting angiogenesis.

During the inflammation process in macrophages treated with LPS, 78 genes were consistently dysregulated at all time points (**Figure 3A**). Interestingly, of these, 76 genes were consistently upregulated (**Figure 3B**), while only two genes, Cyp2u1 and Cbx2, were consistently downregulated. Cyp2u1 encodes an enzyme belonging to the cytochrome P450 superfamily, which catalyzes reactions involved in the synthesis of cholesterol, steroids, and the hydroxylation of fatty acids and their metabolites [32]. It specifically metabolizes arachidonic acid, docosahexaenoic acid, and other long-chain fatty acids, suggesting a role in immune functions [33]. Thus, the downregulation of Cyp2u1 might lead to decreased metabolism of fatty acids, impacting the immune response. Previous studies have shown that upon LPS stimulation, macrophage metabolism shifts from OXPHOS to glycolysis to meet increased energy demands, which includes reduced fatty acid metabolism [29]. These findings suggest that the downregulation of the Cyp2u1 gene is associated with this metabolic shift from OXPHOS to glycolysis, potentially enhancing pro-inflammatory activity in macrophages.

Based on the metabolic changes observed in profile 52 (**Figure 2A**, **2E**), the increased AMPK signaling pathway in profile 41 (**Figure 2A**), and the consistently downregulated gene Cyp2u1, we propose the following hypothesis. In the early stages of the inflammatory response in macrophages challenged by LPS, macrophage metabolism primarily relies on glycolysis to meet the rapidly increasing energy demand. As inflammation progresses to the middle and late stages, the accumulation of metabolites activates key energy metabolism regulators, such as the AMPK pathway, which is triggered by a high ADP (or AMP) to ATP ratio. Consequently, metabolic shifts occur once again during the late middle stage. However, genes regulating fatty acid metabolism, such as Cyp2u1, remain downregulated, so these metabolic changes are primarily associated with amino acid catabolism, as revealed in the GO enrichment analysis of profile 52 (**Figure 2E**).

Regarding the gene Cbx2, previous studies had shown that its expression decreases in macro-

phages upon viral infection consistently over time [34]. However, the role of Cbx2 proteins in innate immunity remains unclear. Subsequent RT-PCR results confirmed the continued decline of these two genes (Cyp2u1 and Cbx2) (**Figure 6A**, **6C**).

To further explore their biological functions during the inflammation process, the consistently upregulated genes (76 genes) underwent GO and KEGG enrichment analyses. These analyses revealed that significantly enriched terms were predominantly associated with inflammation and immunity. STRING analysis also demonstrated that most of these 76 genes formed a tightly interconnected network. The MCODE plug-in of Cytoscape software was utilized to identify the most important module within this network, which consisted of 18 genes. Notably, the majority of these genes exhibit characteristics associated with pro-inflammatory and immune responses, with notable examples including Tnf, Il1b, Il1a, Cxcl10, Cxcl2, and Ccl4. However, an exception was found in the immune responsive gene 1 (Irg1).

Previous research has identified Irg1 as a negative regulator of Toll-like receptor-mediated inflammatory responses through its production of itaconate [35]. Although Irg1 inhibits inflammation by producing itaconate, it also retains a bactericidal function. Prior studies have shown that itaconate exhibits antibacterial properties, notably affecting the glyoxylate shunt in pathogens such as Salmonella typhimurium and Mycobacterium tuberculosis, thus reducing their viability [36]. However, recent studies suggest that Irg1 may also exert pro-inflammatory effects. The depletion of Irg1 in myeloid cells has been shown to reduce inflammatory responses and protect mice against lethal polymicrobial sepsis, indicating a complex role in inflammation that warrants further investigation [37].

To identify potential critical phases in the course of inflammation, we employed WGCNA using time as the trait. We identified three significant modules (pink, red, and turquoise, P-value ≤ 0.01) that correspond to the 1, 3, and 12-hour time points, respectively (**Figure 4B**). Genes with a gene significance (GS) > 0.2 and module membership (MM) > 0.8 within these modules were selected for further analysis. The ClueGO plug-in in Cytoscape software was then used to investigate the biological functions of these key eigengenes. The analysis revealed that the important enrichment GO terms include negative regulation of interleukin-1 beta production, positive regulation of I-κB kinase/NF-κB signaling, and neutral amino acid transmembrane transporter activity at the 1, 3, and 12 h, respectively (**Figure 4C-E**).

These findings suggest that in the inflammatory process of LPS-stimulated macrophages, the critical nodes at 1 and 3 hours are closely associated with the inflammatory response, while the critical node at 12 h is linked to metabolic processes. These observations are consistent with those from the STEM analysis (**Figure 2B-E**). Therefore, our study demonstrates that although the overall process of inflammation undergoes gradual changes, certain time points (1, 3, and 12 h) exhibit significant alterations throughout the inflammatory process. Our work also indicates that the macrophage response to LPS stimulation evolves from the early to the late stages of inflammation, aligning with findings from a previous study [12].

We previously obtained proteomic data at the same time points (except for 1 h) in the same experimental setup [12]. Given that multi-omics analysis provides a more comprehensive view than single-omics approaches, we conducted an integrative analysis of the transcriptomics and proteomics datasets using the "mixOmics" R package. This package facilitates data dimension reduction by employing components that are combinations of all variables, which are instrumental in generating insightful graphical outputs. These outputs help elucidate the relationships and correlation structures between the integrated datasets [22]. In our analysis, the PC1 identified 126 dysregulated genes and 131 dysregulated proteins, which were deemed influential in the macrophage inflammatory response (**Figure 5A**).

Subsequent GO and KEGG enrichment analyses revealed that the majority of the terms associated with the 126 dysregulated genes relate to immune response and metabolism (**Figure 5B**, **5C**). This underscores the alteration in the metabolic profile of macrophages during inflammation, highlighting a close link between metabolism and macrophage func-

tionality, consistent with previous findings [38]. However, the enrichment analysis for the 131 dysregulated proteins primarily related to ribosome biogenesis and metabolism (**Figure 5D**, **5E**). Traditionally viewed as conserved molecular machines without regulatory roles in translation, ribosomes have recently been recognized for their potential regulatory functions. For example, Fujiwara et al. showed that mRNAs preferentially bound by RPL10a/uL1-containing ribosomes require RPL10a/uL1 for efficient translation [39]. Other studies have noted associations between individual ribosomal proteins (RPs) and specific mRNAs, such as RPS25, which is necessary for the efficient translation of C9orf72 and other nucleotide repeats linked to neurodegenerative diseases [40]. O'Neill et al. further demonstrated that RPs perform various regulatory functions in cellular activities, development, and diseases through individual knockdown of 75 RPs [41]. Our previous high-throughput LC-MS/MS analysis also revealed changes in ribosomal protein expression during the inflammatory response of macrophages, suggesting that ribosomes may regulate the inflammatory response in LPS-challenged macrophages through similar mechanisms, offering new insights for future research on inflammation regulation mediated by ribosomal proteins [42].

Finally, our RT-PCR results confirmed the accuracy of our sequencing data, underscoring the reliability of our data analysis.

In summary, this study utilized RNA-seq technology to explore dynamic changes in the transcriptome over time, revealing sequential gene changes that may represent crucial phases in the transition from early to late stages of inflammation. Our findings underscore the pivotal role of metabolism in LPS-challenged macrophages and propose that macrophage metabolism may undergo secondary changes during the middle to late stages of inflammation. The identification of 18 significant DEGs throughout the whole inflammatory response of macrophages stimulated by LPS, along with the crucial role of ribosomes uncovered by multi-omics analysis, provides valuable resources for further investigation into various inflammatory processes. This research will also be instrumental for clinical diagnostics through biomarker gene identification and therapeutic applications by drug target gene screening.

Acknowledgements

This study was supported by grants from the National Natural Science Foundation of China (grant nos. 82272194, 82002089, 82130063 and 82241061), Shenzhen Science and Technology (no. RCBS20210706092252059), Guangdong Basic and Applied Basic Research Foundation (No. 2022B1515120024), and Special Support Plan for Outstanding Talents of Guangdong Province (No. 2019JC05Y340).

Disclosure of conflict of interest

None.

Abbreviations

GEO, Gene Expression Omnibus; DEGs, differentially expressed genes; DEPs, differentially expressed proteins; GO, Gene Ontology; KEGG, Kyoto Encyclopedia of Genes and Genomes; SNP, single-nucleotide polymorphisms; PAMPs, pathogen-associated molecular patterns; RNA-seq, RNA sequencing; LPS, lipopolysaccharide; PRRs, pattern recognition receptors; TLR4, Toll-like receptor 4; MAPK, mitogen-activated protein kinase; TNF, tumor necrosis factor; NF-κB, nuclear factor-κB; AP1, activator protein-1; RT-PCR, quantitative real-time PCR; IRF3, interferon regulatory factor 3; MCODE, molecular complex detection; PRRs, pattern-recognition receptors; TLRs, Toll-like receptors; Irg1, immune responsive gene 1; OXPHOS, oxidative phosphorylation; IL-1, interleukin-1.

Address correspondence to: Yong Jiang, Guangdong Provincial Key Laboratory of Proteomics, State Key Laboratory of Organ Failure Research, Department of Pathophysiology, School of Basic Medical Sciences, Southern Medical University, No. 1023 Shatai South Road, Guangzhou 510515, Guangdong, China. E-mail: jiang48231@163.com

References

[1] Singer M, Deutschman CS, Seymour CW, Shankar-Hari M, Annane D, Bauer M, Bellomo R, Bernard GR, Chiche JD, Coopersmith CM, Hotchkiss RS, Levy MM, Marshall JC, Martin GS, Opal SM, Rubenfeld GD, van der Poll T, Vincent JL and Angus DC. The third international consensus definitions for sepsis and septic shock (Sepsis-3). JAMA 2016; 315: 801-810.

[2] Delano MJ and Ward PA. The immune system's role in sepsis progression, resolution, and long-term outcome. Immunol Rev 2016; 274: 330-353.

[3] Qiu P, Liu Y and Zhang J. Review: the role and mechanisms of macrophage autophagy in sepsis. Inflammation 2019; 42: 6-19.
[4] Huen SC and Cantley LG. Macrophages in renal injury and repair. Annu Rev Physiol 2017; 79: 449-469.
[5] Rogers NM, Ferenbach DA, Isenberg JS, Thomson AW and Hughes J. Dendritic cells and macrophages in the kidney: a spectrum of good and evil. Nat Rev Nephrol 2014; 10: 625-643.
[6] Gordon S and Taylor PR. Monocyte and macrophage heterogeneity. Nat Rev Immunol 2005; 5: 953-964.
[7] Epelman S, Lavine KJ and Randolph GJ. Origin and functions of tissue macrophages. Immunity 2014; 41: 21-35.
[8] Gordon S and Pluddemann A. Tissue macrophages: heterogeneity and functions. BMC Biol 2017; 15: 53.
[9] Luan YY, Dong N, Xie M, Xiao XZ and Yao YM. The significance and regulatory mechanisms of innate immune cells in the development of sepsis. J Interferon Cytokine Res 2014; 34: 2-15.
[10] Lauvau G, Loke P and Hohl TM. Monocyte-mediated defense against bacteria, fungi, and parasites. Semin Immunol 2015; 27: 397-409.
[11] Hamidzadeh K, Christensen SM, Dalby E, Chandrasekaran P and Mosser DM. Macrophages and the recovery from acute and chronic inflammation. Annu Rev Physiol 2017; 79: 567-592.
[12] Schildberger A, Rossmanith E, Eichhorn T, Strassl K and Weber V. Monocytes, peripheral blood mononuclear cells, and THP-1 cells exhibit different cytokine expression patterns following stimulation with lipopolysaccharide. Mediators Inflamm 2013; 2013: 697972.
[13] Chun SC, Jee SY, Lee SG, Park SJ, Lee JR and Kim SC. Anti-inflammatory activity of the methanol extract of moutan cortex in LPS-activated Raw264.7 cells. Evid Based Complement Alternat Med 2007; 4: 327-333.
[14] Wang TS and Deng JC. Molecular and cellular aspects of sepsis-induced immunosuppression. J Mol Med (Berl) 2008; 86: 495-506.
[15] Salomao R, Brunialti MK, Rapozo MM, Baggio-Zappia GL, Galanos C and Freudenberg M. Bacterial sensing, cell signaling, and modulation of the immune response during sepsis. Shock 2012; 38: 227-242.
[16] Wang J, Vodovotz Y, Fan L, Li Y, Liu Z, Namas R, Barclay D, Zamora R, Billiar TR, Wilson MA, Fan J and Jiang Y. Injury-induced MRP8/MRP14 stimulates IP-10/CXCL10 in monocytes/macrophages. FASEB J 2015; 29: 250-262.
[17] Liu Z, Jiang Y, Li Y, Wang J, Fan L, Scott MJ, Xiao G, Li S, Billiar TR, Wilson MA and Fan J. TLR4 signaling augments monocyte chemotaxis by regulating G protein-coupled receptor kinase 2 translocation. J Immunol 2013; 191: 857-864.
[18] Li Z, Scott MJ, Fan EK, Li Y, Liu J, Xiao G, Li S, Billiar TR, Wilson MA, Jiang Y and Fan J. Tissue damage negatively regulates LPS-induced macrophage necroptosis. Cell Death Differ 2016; 23: 1428-1447.
[19] Xu J, Jiang Y, Wang J, Shi X, Liu Q, Liu Z, Li Y, Scott MJ, Xiao G, Li S, Fan L, Billiar TR, Wilson MA and Fan J. Macrophage endocytosis of high-mobility group box 1 triggers pyroptosis. Cell Death Differ 2014; 21: 1229-1239.
[20] Angus DC, Linde-Zwirble WT, Lidicker J, Clermont G, Carcillo J and Pinsky MR. Epidemiology of severe sepsis in the United States: analysis of incidence, outcome, and associated costs of care. Crit Care Med 2001; 29: 1303-1310.
[21] Li L, Chen L, Lu X, Huang C, Luo H, Jin J, Mei Z, Liu J, Liu C, Shi J, Chen P and Jiang Y. Data-independent acquisition-based quantitative proteomics analysis reveals dynamic network profiles during the macrophage inflammatory response. Proteomics 2020; 20: e1900203.
[22] Maier T, Guell M and Serrano L. Correlation of mRNA and protein in complex biological samples. FEBS Lett 2009; 583: 3966-3973.
[23] Liu Y, Beyer A and Aebersold R. On the dependency of cellular protein levels on mRNA abundance. Cell 2016; 165: 535-550.
[24] Haas BJ and Zody MC. Advancing RNA-Seq analysis. Nat Biotechnol 2010; 28: 421-423.
[25] Ekblom R and Galindo J. Applications of next generation sequencing in molecular ecology of non-model organisms. Heredity (Edinb) 2011; 107: 1-15.
[26] Yang SS, Tu ZJ, Cheung F, Xu WW, Lamb JF, Jung HJ, Vance CP and Gronwald JW. Using RNA-Seq for gene identification, polymorphism detection and transcript profiling in two alfalfa genotypes with divergent cell wall composition in stems. BMC Genomics 2011; 12: 199.
[27] Ilut DC, Coate JE, Luciano AK, Owens TG, May GD, Farmer A and Doyle JJ. A comparative transcriptomic study of an allotetraploid and its diploid progenitors illustrates the unique advantages and challenges of RNA-seq in plant species. Am J Bot 2012; 99: 383-396.
[28] Schmelzer C and Doring F. Identification of LPS-inducible genes downregulated by ubiquinone in human THP-1 monocytes. Biofactors 2010; 36: 222-228.
[29] Suzuki T, Hashimoto S, Toyoda N, Nagai S, Yamazaki N, Dong HY, Sakai J, Yamashita T, Nukiwa T and Matsushima K. Comprehensive gene expression profile of LPS-stimulated human monocytes by SAGE. Blood 2000; 96: 2584-2591.

[30] Robinson MD, McCarthy DJ and Smyth GK. edgeR: a Bioconductor package for differential expression analysis of digital gene expression data. Bioinformatics 2010; 26: 139-140.
[31] Anders S and Huber W. Differential expression analysis for sequence count data. Genome Biol 2010; 11: R106.
[32] Yu G, Wang LG, Han Y and He QY. clusterProfiler: an R package for comparing biological themes among gene clusters. OMICS 2012; 16: 284-287.
[33] Ginestet C. ggplot2: elegant graphics for data analysis. J R Stat Soc Ser A Stat Soc 2011; 174: 245-246.
[34] Langfelder P and Horvath S. WGCNA: an R package for weighted correlation network analysis. BMC Bioinformatics 2008; 9: 559.
[35] Rohart F, Gautier B, Singh A and Le Cao KA. mixOmics: an R package for 'omics feature selection and multiple data integration. PLoS Comput Biol 2017; 13: e1005752.
[36] Ernst J and Bar-Joseph Z. STEM: a tool for the analysis of short time series gene expression data. BMC Bioinformatics 2006; 7: 191.
[37] Wang Z, Gerstein M and Snyder M. RNA-Seq: a revolutionary tool for transcriptomics. Nat Rev Genet 2009; 10: 57-63.
[38] Zhang C, Wang G, Wang J, Ji Z, Dong F and Chao T. Analysis of differential gene expression and novel transcript units of ovine muscle transcriptomes. PLoS One 2014; 9: e89817.
[39] Fujiwara N and Kobayashi K. Macrophages in inflammation. Curr Drug Targets Inflamm Allergy 2005; 4: 281-286.
[40] Li L, Zhang Y, Luo H, Huang C, Li S, Liu A and Jiang Y. Systematic identification and analysis of expression profiles of mRNAs and lncRNAs in macrophage inflammatory response. Shock 2018; 51: 770-779.
[41] O'Neill LA and Pearce EJ. Immunometabolism governs dendritic cell and macrophage function. J Exp Med 2016; 213: 15-23.
[42] Mills EL, Kelly B and O'Neill LAJ. Mitochondria are the powerhouses of immunity. Nat Immunol 2017; 18: 488-498.

Table S1. Summary for the transcriptome of macrophages in response to LPS at different time points using Illumina RNA-seq

Sample name	Raw reads	Clean reads	Clean bases	Q20	Q30	GC_rate
RNA_0H-1	22174731	22167667.0	2.22G	0.976422957	0.909650891	0.49370948
RNA_0H-2	16779166	16777306.0	1.68G	0.942510232	0.817211966	0.491175185
RNA_0H-3	21963072	21960177.0	2.20G	0.971956434	0.893876712	0.493822096
RNA_1H-1	22977414	22974263.0	2.30G	0.979712211	0.918648467	0.500412995
RNA_1H-2	26496671	26492916.0	2.65G	0.978606611	0.914413052	0.491301966
RNA_1H-3	21523089	21517583.0	2.15G	0.978852426	0.915616123	0.494358347
RNA_3H-1	29593713	29589830.0	3.00G	0.979078396	0.915313379	0.490136099
RNA_3H-2	21955827	21948046.0	2.20G	0.977349689	0.910534197	0.492060157
RNA_3H-3	22566750	22563250.0	2.26G	0.971211002	0.891274251	0.492458552
RNA_6H-1	25449011	25445238.0	2.54G	0.978612304	0.915488365	0.494050156
RNA_6H-2	24286655	24283035.0	2.43G	0.975148345	0.903076186	0.498134137
RNA_6H-3	26061588	26058283.0	2.61G	0.979903367	0.918507606	0.497953011
RNA_12H-1	23249622	23246894.0	2.32G	0.969392553	0.887212181	0.496203502
RNA_12H-2	23616581	23612632.0	2.36G	0.976922439	0.908771698	0.496939861
RNA_12H-3	19776064	19765696.0	1.98G	0.978070569	0.91418803	0.496222169
RNA_24H-1	18805445	18801043.0	1.88G	0.953476431	0.843826152	0.501629703
RNA_24H-2	26552977	26549616.0	2.66G	0.976551446	0.907672509	0.495954053
RNA_24H-3	26310005	26306536.0	2.63G	0.979119999	0.916406168	0.498539313

Table S2. Summary of clean reads mapped to the reference macrophage genome (mouse)

Sample name	Total reads	Mapped reads	Mapped ratio
RNA_0H-1	22167667.0	18411096	83.05%
RNA_0H-2	16777306.0	13829697	82.43%
RNA_0H-3	21960177.0	16990462	77.37%
RNA_1H-1	22974263.0	19910395	86.66%
RNA_1H-2	26492916.0	22122206	83.50%
RNA_1H-3	21517583.0	18314018	85.11%
RNA_3H-1	29589830.0	24594881	83.12%
RNA_3H-2	21948046.0	17575435	80.08%
RNA_3H-3	22563250.0	18406879	81.58%
RNA_6H-1	25445238.0	19861379	78.06%
RNA_6H-2	24283035.0	20652759	85.05%
RNA_6H-3	26058283.0	22126179	84.91%
RNA_12H-1	23246894.0	19948690	85.81%
RNA_12H-2	23612632.0	20072830	85.01%
RNA_12H-3	19765696.0	16724484	84.61%
RNA_24H-1	18801043.0	15808418	84.08%
RNA_24H-2	26549616.0	21990660	83.23%
RNA_24H-3	26306536.0	21990660	83.59%

Table S3. Primers for amplification of the genes

Gene name	Forward primer sequence	Reverse primer sequence
Cyp2u1	TCGCCATTCCTCACATGACCTC	CGATGAGGACAGAAGTCGTCTG
Cbx2	CATGAGAAGGAGGTTCAGAACCG	GAGGACGAACTGCTGGATTTGG
Irg1	GGTATCATTCGGAGGAGCAAGAG	ACAGTGCTGGAGGTGTTGGAAC
Creb3l2	TCGAACCTGCAAGTTAGCTGGC	AGCCATCTTGGTGGCAGAAGGA
β-actin	CCTCTATGCCAACACAGTGC	CCTGCTTGCTGATCCACATC
Spp1	GCTTGGCTTATGGACTGAGGTC	GCTTGGCTTATGGACTGAGGTC
Slc15a3	CTTGCGTTCCAAAACTGCTGTCC	TTCACCAGCACCTGGAAGTTGG

Network profiles of mRNA in macrophages challenged with LPS

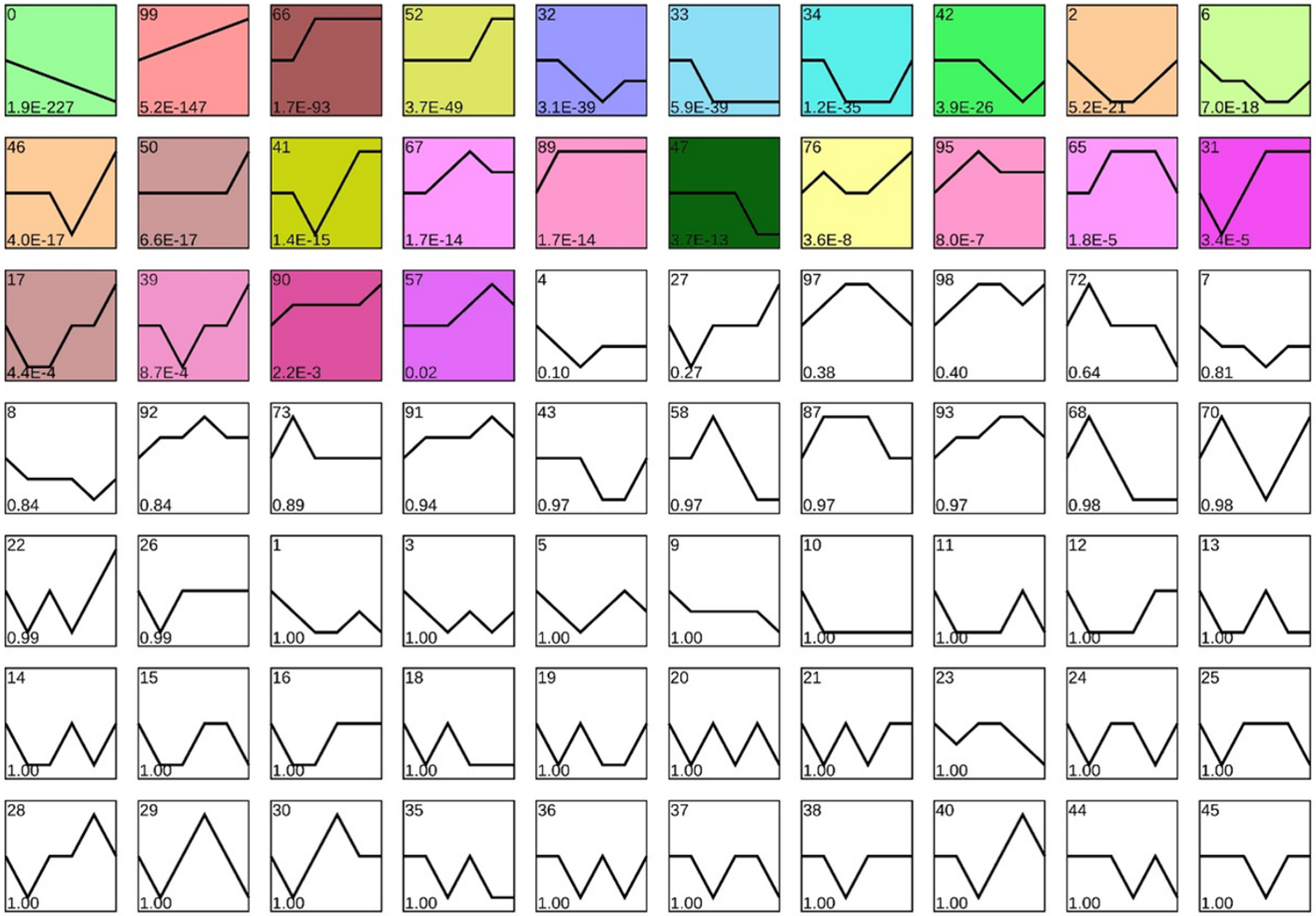

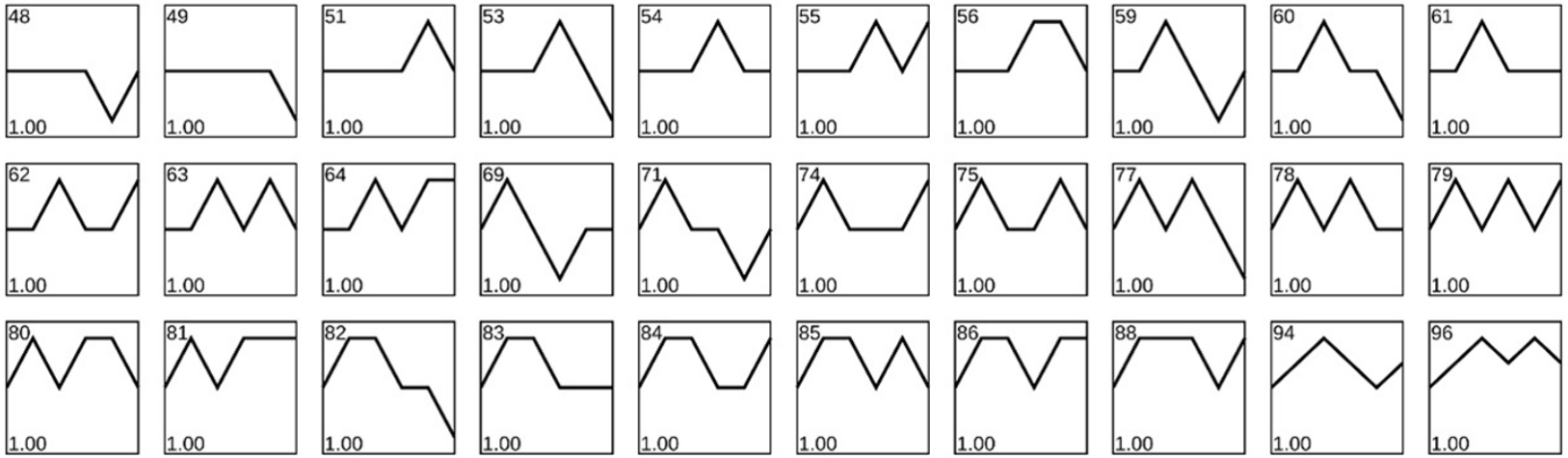

Figure S1. Profiles ordered based on the *P* value significance of number of genes assigned versus expected.

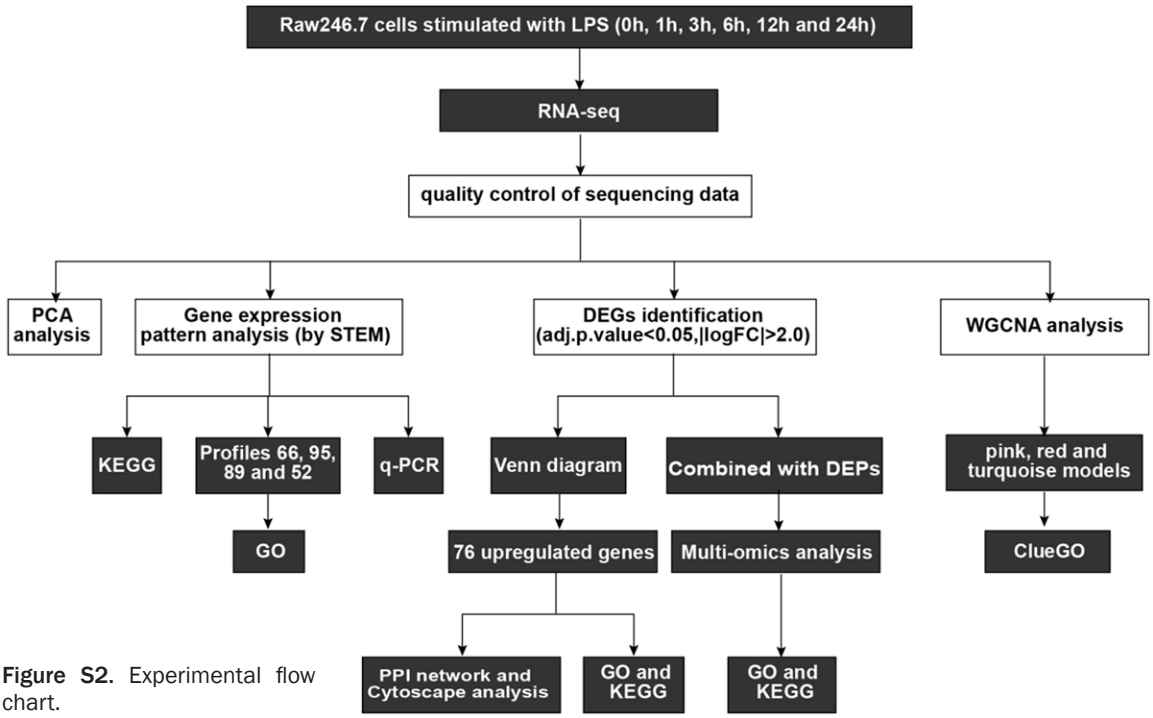

Figure S2. Experimental flow chart.

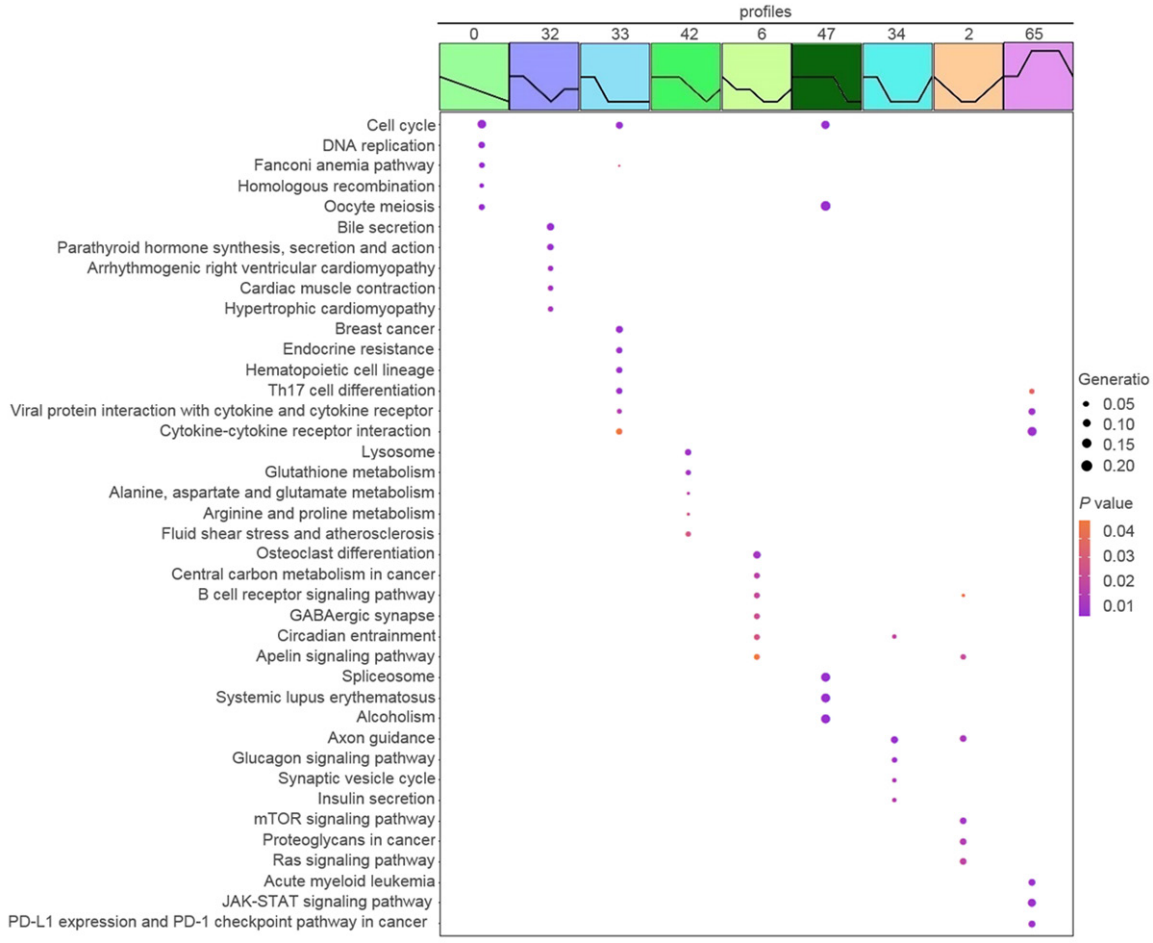

Figure S3. Patterns of global temporal changes in genes of category B and category C abundance during the inflammatory process of macrophages challenged with LPS.

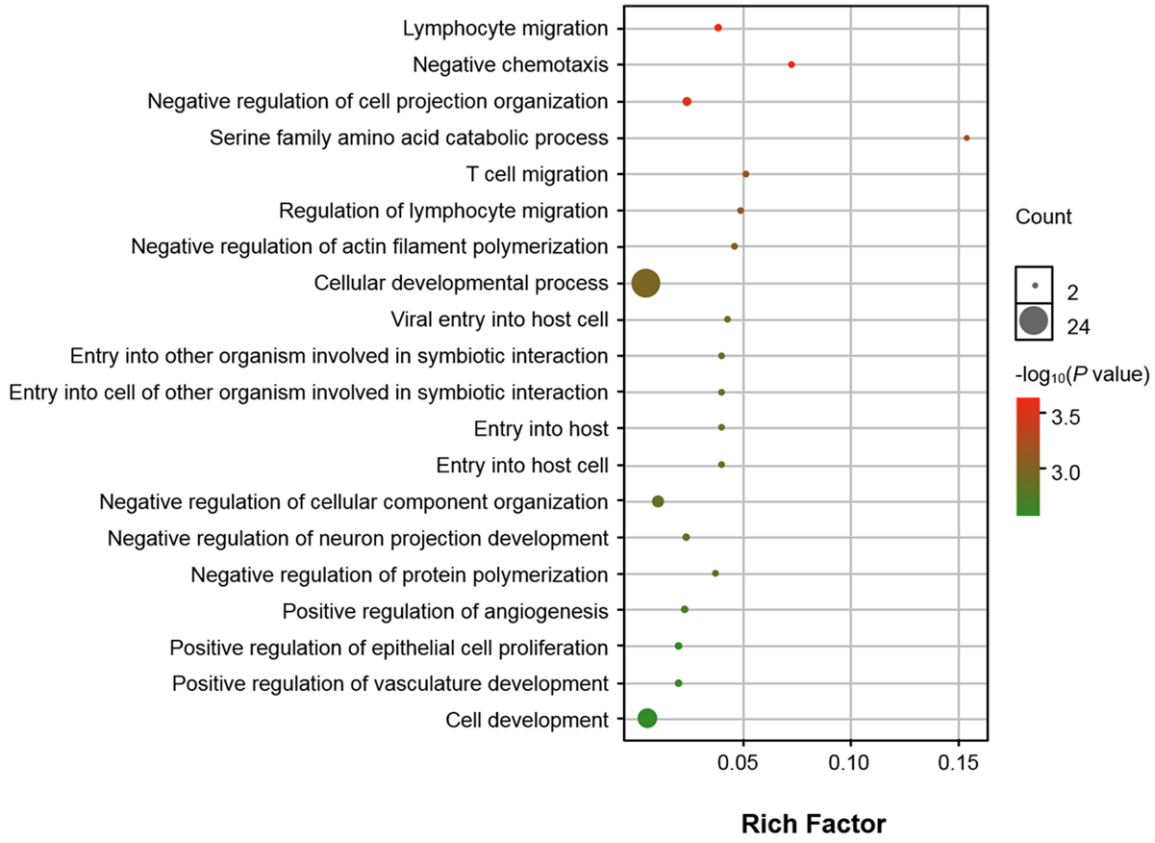

Figure S4. Top 20 GO enrichment terms in profile 50 discloses gene regulatory networks governing biologic function.